Quantum molecular dynamics simulation of multifragment production in heavy ion collisions at $E/A=600$ MeV

M. Begemann-Blaich,[1] W. F. J. Müller,[1] J. Aichelin,[2] J. C. Adloff,[4] P. Bouissou,[5] J. Hubele,[1] G. Imme,[6] I. Iori,[7] P. Kreutz,[3] G. J. Kunde,[1] S. Leray,[5] V. Lindenstruth,[1] Z. Liu,[1,*] U. Lynen,[1] R. J. Meijer,[1,†] U. Milkau,[1] A. Moroni,[7] C. Ngô,[5] C. A. Ogilvie,[1] J. Pochodzalla,[1] G. Raciti,[6] G. Rudolf,[4] H. Sann,[1] A. Schüttauf,[3] W. Seidel,[8] L. Stuttge,[4] W. Trautmann,[1] and A. Tucholski[1,‡]

[1]*Gesellschaft für Schwerionenforschung, D-6100 Darmstadt, Germany*
[2]*Laboratoire de Physique Nucléaire, F-44072 Nantes, France*
[3]*Institut für Kernphysik, Universität Frankfurt, D-6000 Frankfurt, Germany*
[4]*Centre de Recherches Nucléaires, F-67037 Strasbourg, France*
[5]*Laboratoire National Saturne, CEN Saclay, F-91191 Gif-sur-Yvette, France*
[6]*INFN, Dipartimento di Fisica dell'Universitá, I-95129 Catania, Italy*
[7]*INFN, Istituto di Scienze Fisiche, Universita degli Studi di Milano, I-20133 Milano, Italy*
[8]*Forschungszentrum Rossendorf, O-8051 Dresden, Germany*

(Received 17 February 1993)

With the ALADIN forward spectrometer the fragmentation of gold nuclei at 600 MeV per nucleon after interaction with carbon, aluminum, copper, and lead targets has been investigated. The results are compared to quantum-molecular-dynamics (QMD) calculations using soft and hard equations of state as well as a soft equation of state with momentum-dependent forces. Whereas the QMD has been successfully applied to heavy ion collisions at lower energies, it is not possible to reproduce the fragment distributions and the light-particle multiplicities observed in this experiment at relativistic energies. To study the reasons for the discrepancy between the experimental data and the simulations we investigated the time evolution of the nuclear system after a collision and the disintegration pattern of excited nuclei in the QMD approach.

PACS number(s): 25.70.Pq

I. INTRODUCTION

The decay mechanism of a nucleus with an excitation energy comparable to its total binding energy is one of the open questions in nuclear physics. It has been shown by previous experiments [1–4] that in this energy regime between the region of particle evaporation and that of total disassembly the production of several intermediate mass fragments is the dominant decay channel. Many theoretical scenarios have been proposed to describe this decay channel of a nucleus at intermediate excitation energies. They range from a nearly simultaneous breakup due to large fluctuations in regions of mechanical instability [5,6] to statistical multifragmentation models which calculate the available phase space for the simultaneous decay of an expanded nuclear system [7,8], and sequential decay processes where equilibrium is reestablished after each binary decay [9–12]. A comparison of our data with these nonmicroscopic descriptions has been published elsewhere [13,14]. Both statistical fragmentation models and the rapid massive cluster formation model [12] can reproduce our measured multiplicity distributions. However, this is unsatisfactory because all of these calculations are based on hybrid models which require coupling to a dynamical model and assume the existence of equilibrium prior to the fragmentation process. Therefore the dynamical properties of the primary stage of a reaction are neglected and fluctuations are not taken into account.

Here we compare our experimental data with the results of the quantum-molecular-dynamics (QMD) model developed by Stöcker and Aichelin [15] in the version by Aichelin and co-workers [16]. The QMD model is a dynamical model which was developed to follow the reaction process on a microscopical basis. It describes the reaction dynamics of heavy ion collisions from the initially separated projectile and target nuclei up to the final formation of fragments. The combined target-projectile system is propagated microscopically using as input the experimental free scattering cross sections as well as a variety of representations for the forces between nucleons resulting in different nuclear equations of state. An agreement of experiment and theory only means that a set of parameters exists that can reproduce the data. More interesting are, however, any discrepancies because they may imply that the description of the reaction dynamics is incorrect or alternatively that the input parameters of the model are wrong. This offers the possibility to explore new physics like—for example—the

*Present address: Institute of High Energy Physics, 100039 Peijing, People's Republic of China.
†Present address: PTT Research, NL-9700 Groningen, Netherlands.
‡Present address: IPJ Swierk, PL-05-400 Swierk, Otwoc, Poland.

modification of the free cross section in medium. To investigate discrepancies in detail and to discuss possible reasons is the aim of this paper.

II. EXPERIMENTAL SETUP

The experiment was performed with the ALADIN spectrometer at SIS, using a gold beam of 600 MeV/nucleon and carbon, aluminum, copper, and lead targets. A detailed description of the apparatus was given in Ref. [1]. The charge and the velocity of fragments with $Z \geq 2$ were determined with a time-of-flight wall positioned 6 m downstream of the target. The time-of-flight (TOF) wall covered an area of 1 m $\times$ 1.1 m with two layers of 40 scintillators each. For fragments with beam velocity and an N/Z ratio of 1 this corresponds to an angular acceptance of $\pm 4.7°$ in the horizontal and $\pm 4.5°$ in the vertical direction. This is sufficient to detect all fragments with $Z \geq 6$ originating from the decay of the gold projectile, since in inverse kinematics these particles are strongly forward focused. For $Z = 3$, 4, and 5 the acceptance is still above 95% except for fragments in central collisions [1]. Unit charge resolution was obtained for $Z \leq 8$ and a resolution of two charge units for the heavier elements.

The multiplicity of light charged particles, predominantly protons emitted from the midrapidity source, was determined by the 64 elements of a Si-CsI(Tl) forward hodoscope. The detectors were placed at angles between 7° and 40° with a solid angle coverage of approximately 30%. Due to the thickness of the Si detectors the energy threshold for particle identification in the hodoscope was 10 MeV/nucleon, which is far below the average energy of midrapidity particles. The energy of these particles, however, was not determined because midrapidity protons and α particles were not stopped in the detectors.

III. QMD CALCULATIONS

A. Details of the code

The quantum-molecular-dynamics model and the quasiparticle dynamics (QPD) model by Boal and Glosli [17] are presently the only models that describe the fragment formation in a dynamic microscopical framework. Here, we compare the observed fragment distributions with the prediction of the QMD code. We want to summarize only briefly the relevant properties of the code. For more details the reader is referred to [16].

Each single nucleon of the two colliding nuclei is described by a Gaussian in momentum and coordinate space. At the beginning, the nuclei move along Coulomb trajectories. As soon as the distance between the surfaces of the two nuclei is below 2 fm and hence the nuclear interaction sets in, the centroids of the Gaussians are propagated under the influence of mutual two- and three-body interactions.

The interaction is chosen as a local Skyrme-type interaction which was used frequently in time-dependent Hartree-Fock (TDHF) calculations and has been proven to reproduce the static properties of nuclei. Two parametrizations—labeled "hard" and "soft"—are used which yield a different compressibility of nuclear matter, supplemented by a long-range Yukawa interaction and an effective Coulomb interaction. To take into account the momentum dependence of the nuclear interaction, a momentum-dependent contribution can be added as an option, which is adjusted to the experimentally determined momentum dependence of the optical potential.

For the scattering of nucleons in nuclear matter at high energies, the influence of the Pauli blocking is small and the Brückner G matrix becomes identical to the transition matrix which describes the scattering between free nucleons. Therefore, the Pauli blocking of the intermediate states is neglected and only that of the final states is included. As the in-medium corrections to the nucleon-nucleon cross sections are not known, the calculations are done with the measured free elastic and inelastic nucleon-nucleon cross sections which were parametrized by Cugnon [18]. The Pauli blocking of the final states is determined by the overlap of the two nucleons in phase space with all other nucleons. The collision is then allowed with a probability $P=(1-P_1)(1-P_2)$, where P_1 and P_2 are the fractions of the final phase space which are already blocked by other nucleons. If a collision is blocked, the momenta of the scattering partners prior to the scattering are restored.

B. Details of the calculations

For a systematic study, we generated several thousand events for the reaction of gold projectiles with the four targets of carbon, aluminum, copper, and gold. (The calculations were performed using gold instead of lead to reduce the CPU time needed by a factor of 2: If a symmetric system is studied each simulated event can be used twice by exchanging the role of the target and the projectile nucleus.) The impact parameter was varied with a flat distribution between 0 and an upper limit between 10 and 14 fm depending on the size of the target nucleus. Three different equations of state (EOS) were used: a soft EOS with a nuclear compressibility K of 200 MeV, a hard EOS with $K=380$ MeV, and a soft EOS with $K=200$ MeV and momentum-dependent interactions (MDI). For 24 time steps (starting at 0.2 up to 300 fm/c after the beginning of the collision) the momenta and the positions of all nucleons were stored and for each of these time steps the spatial distribution of the nucleons was investigated to examine the formation of clusters. In our definition, two nucleons are members of the same cluster if the distance of their centroids in coordinate space is smaller than the cluster parameter d_0. To check the influence of the exact value of d_0 on the final cluster distributions, d_0 was varied between 1.0 and 4.0 fm. It turned out that for all values above 2.5 fm the distributions at the end of the time evolution were the same, therefore a value of 3.0 fm was used. After 300 fm/c, the calculations were stopped assuming that the cluster formation was finished by that time.

Since the QMD simulation does not distinguish between neutrons and protons, a charge had to be assigned to each cluster. Complex fragments with mass 2 and above and a rapidity above midrapidity were assumed to

stem from the projectile and their charge was calculated using the N/Z ratio of the projectile, whereas for complex fragments with a rapidity below midrapidity the N/Z ratio of the target nucleus was used. The remaining charge was distributed randomly among the nucleons with mass 1. The resulting charged clusters were sent through a software experiment filter to simulate the acceptance and the granularity of our apparatus as well as the deflection by the ALADIN magnet. This is most important for the investigation of midrapidity particles since the geometrical acceptance of our apparatus for those particles is significantly smaller than 100%.

IV. COMPARISON WITH EXPERIMENTAL DATA

A. The projectile spectator

The process of multifragmentation is known to be the dominant decay channel in the excitation energy regime between the region of particle evaporation and that of total disassembly [1–4]. Any quantitative study of the conditions that lead to the emission of several intermediate mass fragments requires therefore the knowledge of the violence of the collision, i.e., of the impact parameter. In the participant-spectator model the size of the projectile spectator—measured via the total charge of all nuclear fragments with velocities near the projectile velocity—would be a possible measure of the centrality of a collision. In our experiment protons originating from the projectile spectator were not detected, therefore the similar quantity Z_{bound}, the sum of all charges of projectilelike fragments with $Z \geq 2$, was constructed. It was shown [1] that Z_{bound} allows a very good determination of the impact parameter. Z_{bound} is thus a measure of the violence of the collision and of the energy deposited in the excited spectator.

In the following we want to discuss the correlation between three observables and Z_{bound}: Z_{max} is the charge of the largest projectile fragment, M_{IMF} is the multiplicity of intermediate mass fragments (IMF) with $3 \leq Z \leq 30$, and M_{lp} is the multiplicity of light charged particles detected in the Si-CsI hodoscope. M_{IMF} signals the onset of multifragment emission from the projectile spectator whereas Z_{max} gives some insight how the projectile spectator breaks apart. M_{lp}, on the other hand, contains information about the participant zone of the nuclear reaction, though for asymmetric nuclear reactions and central collisions—where target and projectile overlap completely—M_{lp} is rather insensitive to the impact parameter [19,1].

Figure 1 shows the correlation between Z_{max} and Z_{bound} for the experimental data (left) and the QMD simulations (right). By definition Z_{bound} is always larger than or equal to Z_{max}, therefore all events are located below the diagonal. Events with a value of Z_{bound} near $Z_{\text{projectile}}$, i.e., very peripheral collisions, which have at the same time a Z_{max} of approximately half of the projectile charge are binary fission events. Points on the diagonal correspond to events where only one fragment has been detected; points in the vicinity of the diagonal

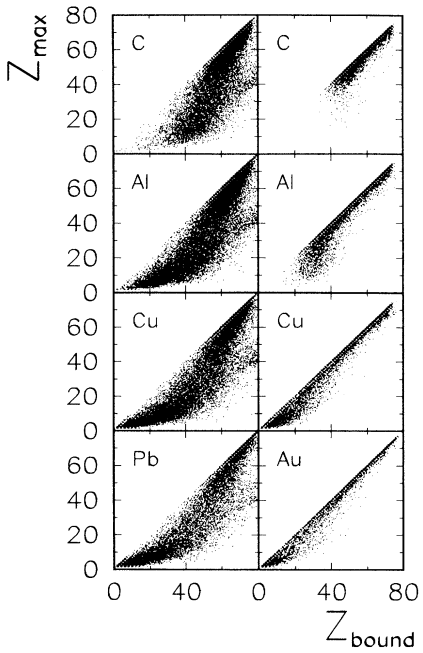

FIG. 1. Left: Correlation between the largest projectile fragment Z_{max} and Z_{bound} for Au+C, Au+Al, Au+Cu, and Au+Pb reactions at $E/A = 600$ MeV. Right: Correlation between Z_{max} and Z_{bound} for Au+C, Au+Al, Au+Cu, and Au+Au calculations using a soft EOS without MDI. Whereas the data show a broad distribution of Z_{max} for values of Z_{bound} around 50, the simulations predominantly predict one large fragment for all values of Z_{bound}.

represent typical evaporation events where at least two fragments have been observed but most of the charge is concentrated in one of them. For values of Z_{bound} around 50, a rapid decrease of Z_{max} is observed, indicating a transition to events where the charge is distributed more equally over two or more fragments. For the heavier targets a sizable part of the cross section is still found in a region where both Z_{max} and Z_{bound} are small. These are processes where so much excitation energy is deposited in the spectator matter that the total disassembly into mostly nucleons and a few light fragments will occur [1,20].

The events from the QMD calculations with a soft EOS show a different behavior. For all values of Z_{bound}, Z_{max} is fairly close to Z_{bound}. This means that one heavy fragment survives and that the number of intermediate mass fragments is small. Especially, the simulation fails to predict the rapid decrease of Z_{max} for Z_{bound} values of approximately 50.

In Fig. 2, the mean multiplicity of IMF's is plotted versus Z_{bound} for the experimental data as well as QMD simulations using a soft EOS. The mean multiplicity observed within the acceptance of the ALADIN spectrometer is first increasing with decreasing Z_{bound} up to a maximum value of 3.5 to 4 at $Z_{\text{bound}} \approx 40$. For smaller values of Z_{bound}, corresponding to more central collisions, the IMF multiplicity is again decreasing. Except for a weak systematic decrease of the maximum multiplicity with increasing mass of the target nucleus, a remarkable target

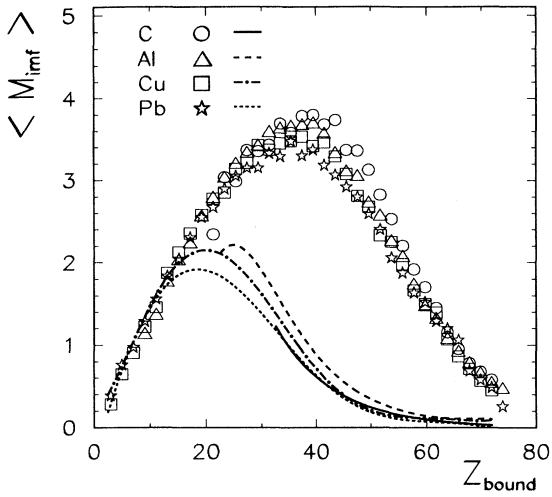

FIG. 2. Correlation between the mean IMF multiplicity $\langle M_{IMF} \rangle$ and Z_{bound}. Symbols: experimental data for the systems Au+C, Au+Al, Au+Cu, and Au+Pb at $E/A=600$ MeV. Lines: QMD calculations for the systems Au+C, Au+Al, Au+Cu, and Au+Au using a soft EOS. The simulations significantly underestimate the IMF production.

independence is found. The corresponding distributions for the simulated events reproduce the target independence, they, however, significantly underestimate the production of intermediate mass fragments, as was already seen in Fig. 1. Moreover, the maximum is shifted to much smaller values of Z_{bound}. This indicates that for the QMD events the maximum of the IMF production is reached at more central collisions.

To investigate this, we plotted the mean IMF multiplicity as well as the mean Z_{max} versus the impact parameter b of the collisions. For the experimental data the geometrical cross-section method was applied to the Z_{bound} distributions in order to reconstruct the impact parameter [1]. For the simulations the impact parameter is known. The left side of Fig. 3 shows the mean IMF multiplicity for the experimental data (open symbols) and the QMD calculations (solid symbols). Indeed, in the simulations the maximum of the IMF multiplicity is reached for significantly smaller values of b than in the experimental data. At the same time the biggest fragment emerging at a given impact parameter is much larger as can be seen in the right part of Fig. 3. The discrepancy for the mean IMF multiplicity is getting less pronounced with increasing mass of the target nucleus. This is partly due to the definition of IMF's: As soon as Z_{max} falls below 30 the multiplicity of IMF's increases by one unit. While in the case of the carbon target the mean Z_{max} is above 30 for all impact parameters, Z_{max} decreases to smaller values than 30 for the heavier targets and small impact parameters. The figure illustrates once more the fact that in the QMD simulations the spectator matter does not break into several IMF's but stays together as one big cluster in contradiction to the experiment.

Since the IMF multiplicity distribution as a function of Z_{bound} is independent of the target for both the experimental data and the calculations using a soft EOS, the different EOS's were only studied for the system Au on Cu. Figure 4 shows the data together with the two choices for the EOS. The difference between the soft and the hard EOS without MDI is only marginal.

We also investigated the soft EOS with a momentum-dependent interaction. It turned out that the disintegra-

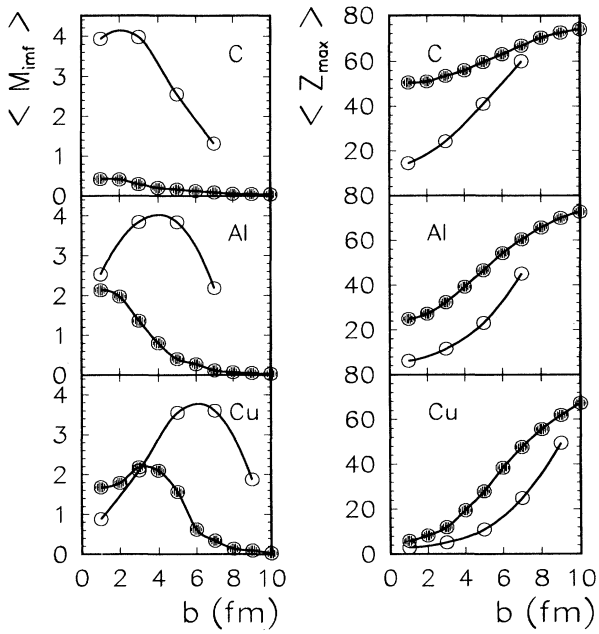

FIG. 3. Mean IMF multiplicity (left) and mean Z_{max} (right) vs the impact parameter b, for both the experimental data (open circles) and the QMD calculations (solid circles). For the simulations the maximum of the IMF multiplicity is reached for significantly smaller values of b. At the same time the biggest fragment for a given impact parameter is much larger than for the experimental data. Top, Au+C; middle, Au+Al; bottom, Au+Cu at 600 MeV/nucleon. The lines were drawn to guide the eye.

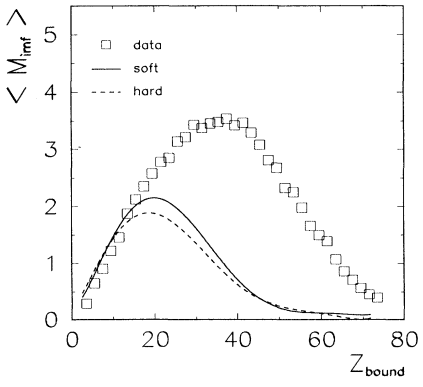

FIG. 4. Correlation between the mean IMF multiplicity $\langle M_{IMF} \rangle$ and Z_{bound} for Au+Cu reactions at $E/A=600$ MeV. Symbols, experimental data; solid line, soft EOS; dashed line, hard EOS. The difference of the results obtained with the two EOS's is only marginal.

tion pattern of nuclei with and without MDI is very different: For the soft EOS without MDI, target and projectile remain stable with respect to the emission of IMF's and evaporate at most a few nucleons or α particles down to impact parameters of approximately 9 fm. This contrasts sharply with the results for the soft EOS with MDI, where the clusters have a high probability to decay via the emission of IMF's even for the largest impact parameters. The lighter target spectator especially completely disintegrates into small fragments. The relatively high IMF multiplicities found for the EOS with MDI are in better agreement with the experimental findings than the results obtained with the EOS's without MDI. This effect is not unexpected because it is known that momentum-dependent interactions yield a larger momentum transfer. However, a word of caution has to be added: The additional momentum dependence increases the numerical error of the integration routines from $O(\Delta t^2)$ to $O(\Delta t)$, where Δt is the time step chosen for the integration [16]. Momentum-dependent interactions therefore produce nuclei which are numerically less stable from the beginning, and an unknown part of the fragment production produced is hence artificial. So to use a parametrization of the nuclear EOS with a momentum-dependent contribution may be a promising approach, but any comparison with experimental results has to wait until the attempts to obtain numerically stable solutions for this description of nuclei will be successfully completed.

B. The participant zone

So far, only the decay of the projectile spectator was examined. The QMD model is also able to describe the participant zone of the reaction. Consequently, the mean multiplicity of light charged particles $M_{\rm lp}$, predominantly protons and α particles, detected in the forward hodoscope was also studied as a function of $Z_{\rm bound}$. Figure 5 (top) shows the experimental data for all targets together with the calculations for a soft EOS. In Fig. 5 (bottom), the Cu data are compared to the results of both QMD calculations. Again the differences between the hard and the soft EOS are only small. All simulations predict multiplicities which are about 20% below the experimental values.

Due to our incomplete angular coverage for midrapidity particles, small differences in the angular distributions of light charged particles for the experimental data on the one hand and the simulated events on the other hand could easily lead to discrepancies in the number of detected charged particles even if the total cross sections were in good agreement. We therefore studied the differential cross sections $d\sigma/d\Omega$ for both the experimental data and the calculations using the soft EOS. The results are shown in Fig. 6: The shapes of the experimental and theoretical distributions are very similar for all systems studied. The differences seen in the light-particle yields at midrapidity must therefore be attributed to a smaller total production cross section.

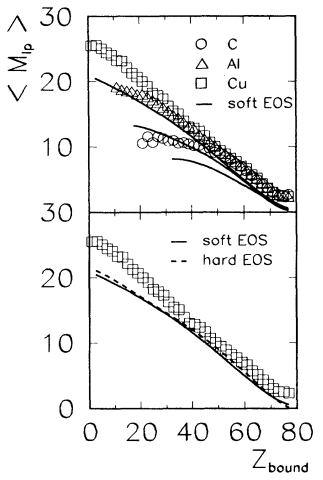

FIG. 5. Top: Correlation between the mean multiplicity of light charged particles $\langle M_{\rm lp} \rangle$ and $Z_{\rm bound}$ for Au+C, Au+Al, and Au+Cu reactions at $E/A=600$ MeV. Symbols, experimental data; lines, QMD calculations using a soft EOS. Bottom: Correlation between the mean multiplicity of light charged particles $\langle M_{\rm lp} \rangle$ and $Z_{\rm bound}$ for Au+Cu reactions. Symbols, experimental data; solid line, soft EOS; dashed line, hard EOS. The simulations predict multiplicities of light charged particles which are approximately 20% below the experimental values.

V. BEHAVIOR OF QMD NUCLEI

In Sec. IV, we presented some evidence that heavy ion collisions at relativistic energies are not described properly by the QMD version used. The discrepancies between the experimental results and the simulations may be due to three reasons: (i) the intermediate mass fragment formation is not finished by the time the calculations are stopped, (ii) the emission of several intermediate mass fragments is not a dominant decay channel for excitation energies comparable to the total binding energy of the

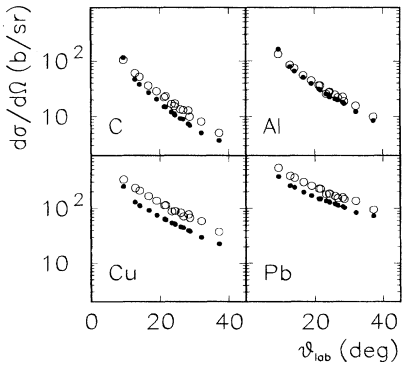

FIG. 6. Differential cross sections of light charged particles for Au+C, Au+Al, Au+Cu, and Au+Pb reactions at $E/A=600$ MeV. Large open symbols, data; small solid symbols, QMD calculations using a soft EOS. For all systems, the shapes of the experimental and theoretical angular distributions are very similar.

spectator, and (iii) the collision process is not described properly and the energy transfer from the participants to the spectators is not sufficient. In this section we want to investigate these possibilities in more detail.

A. Time evolution of the QMD system after a collision

In order to check whether the deexcitation of the reaction products is completed after 300 fm/c, we studied the time evolution of the system Au on Cu for a soft EOS after a collision. The following procedure was used: In the last step of the calculation a cluster of a specific size was selected. The history of its constituent nucleons was followed backwards in time and for each time step the preceding cluster was determined which contained the majority of these nucleons. This procedure is only meaningful if the exchange of nucleons between separated clusters is small. But it turned out that the preceding clusters contain between 80 and 100 % of the nucleons of the final cluster. For the nucleons of each precluster, their binding energy was calculated as the sum of their potential energy and their kinetic energy with respect to the center of mass of the precluster was calculated. At the same time the size of each precluster was determined. This investigation was done for final clusters of all sizes which contained predominantly projectile nucleons—for light fragments with masses between 10 and 20 up to heavy residues in the vicinity of the projectile nucleus. The results are shown in Fig. 7 for the mass intervals 10–20, 40–50, 70–80, and 120–130. The top panel shows the development of the average binding energy in time. After approximately 100 fm/c the preclusters are practically cold, they have a binding energy of the order of 8 MeV/nucleon. At the same time the cluster formation has almost finished. This is illustrated in Fig. 7 (bottom)

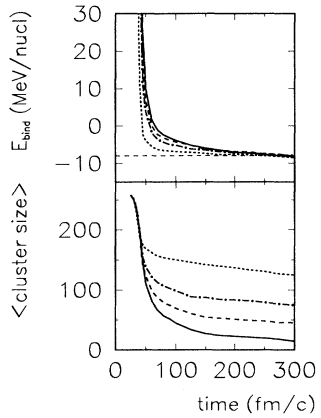

FIG. 7. Time development of the system Au on Cu for soft EOS. Top: Average binding energy per nucleon for fragments from the projectile spectator which, in the last time step, have a mass number between 10 and 20 (solid line), 40 and 50 (long-dashed line), 70 and 80 (dash-dotted line), 120 and 130 (short-dashed line). The horizontal dashed line indicates a binding energy of 8 MeV/nucleon. Bottom: Mean number of nucleons for clusters which have in the last time step a mass between 10 and 20, 40 and 50, 70 and 80, 120 and 130. After a time interval of 100 fm/c all fragments, independent of their size, are practically cold and the fragment formation process is completed.

where the mean size of the preceding clusters is plotted for the same mass bins. The breakup of the excited projectile spectator into smaller fragments is over after 100 fm/c and from there on only a few nucleons are evaporated. This means that, in the framework of this code, the deexcitation of the heated nuclear matter via the emission of fragments is finished after 100 fm/c, the remaining clusters are practically cold and the eventual further deexcitation will therefore proceed dominantly via γ emission.

B. Single excited QMD nuclei

In a next step we performed studies of the decay of an excited QMD nucleus. Instead of exciting the nucleus via a (dynamic) collision process, a certain amount of kinetic energy was given to all its nucleons directly after the initialization. It is a simplification to study the disintegration pattern of only spherical nuclei since heavy ion collisions may produce far more complicated shapes. However, the QMD decay modes can be compared to those of statistical models which retain this symmetry. Since those models include in more detail nuclear properties, like level densities, etc., a comparison may be useful and it may be especially possible to evaluate whether the thermal properties of the QMD approach are correct.

1. Generation of excited QMD nuclei

The total kinetic energy of a cold QMD nucleus directly after its initialization was calculated. A fixed amount of excitation energy was added to this value by increasing the momenta of all nucleons by a constant scaling factor, i.e., an instantaneous energy deposition, that changes the momenta of all nucleons at the same time and by the same factor is assumed. This is a very simple method to simulate an excited nucleus. However, in this way one does not create a heated nucleus in thermal equilibrium: In the latter case the nuclear density would be reduced, moreover, the occupation probability for the states with the lowest momenta would not be modified significantly while, on the other hand, much higher maximal momenta would occur due to the softening of the Fermi surface. This means, in particular, that it is not possible to assign a temperature to this nuclear cluster. But real collisions in nature will also not initially produce heated clusters in thermal equilibrium. During the time evolution of the nucleus, the system will develop towards thermal equilibrium. Nucleon-nucleon collisions were completely suppressed for this study because the few collisions which are not forbidden by the Pauli principle do not influence the results significantly.

For each of the three EOS's discussed earlier, 2000 gold nuclei with excitation energies between 0 and 20 MeV/nucleon were produced and their evolution in time was followed. Additionally, the same amount of xenon and zirconium nuclei was created for a soft EOS only to allow for comparisons between different system sizes. The calculations were performed using the same time steps as before. Again the cluster algorithm together with the charge assignment was applied for each of these time steps.

2. *Decay of the excited nuclei*

The deexcitation of the nuclei which were excited as described above was then investigated. First, we studied the production of IMF's as a function of the excitation energy given to a gold nucleus at rest. Figure 8 (top) shows the correlation between the mean IMF multiplicity and the excitation energy per nucleon for gold nuclei. Depending on the EOS used, maximum mean multiplicities as high as 5 or 8 are found. The corresponding excitation energies vary from 12.5 MeV/nucleon for the hard EOS to 10.0 MeV/nucleon for the soft EOS.

For the soft EOS, nuclear systems with different sizes were compared. In Fig. 8 (bottom), the mean IMF multiplicity per nucleon versus the excitation energy per nucleon is plotted for gold, xenon, and zirconium nuclei. Within the statistical errors, the mean number of IMF's normalized to the size of the nucleus for a given excitation energy per nucleon is independent of the size of the system.

In Fig. 9, we compare the relation between excitation energy and IMF production found for QMD using a soft EOS with the results of the standard statistical multifragmentation calculations by Gross [21]. (For details of this calculation see Hubele *et al.* [13].) Although the approaches are very different, the QMD calculations are in qualitative agreement with the results of the statistical model. A more detailed comparison to other statistical models and the rapid massive cluster formation (RMCF) model by Friedman [11,12] has been published elsewhere [22].

The results of this section cannot be directly compared to the experimental data because in a real collision the size of the decaying projectile spectator as well as the energy deposited during the collision process is changing with the centrality of the reaction, while in the calculations the size of the decaying system was fixed. Nonetheless, we tried to get at least an estimate for the correlation between the mean IMF multiplicity and Z_{bound}: In the framework of the participant-spectator model it is possible to calculate the size of the spectator for a given nuclear system at known impact parameter using only very simple geometrical assumptions [23]. The relation between the excitation energy and the impact parameter, on the other hand, is strongly dependent on the model used. Here, we adopted the same approach as for the hybrid calculations of Hubele *et al.* [13], i.e., the excitation energy was varied between 25 and 0 MeV/nucleon for an impact parameter interval of 0–10 fm according to the results of Boltzmann-Uehling-Uhlenbeck (BUU) calculations [20,24]. These two pieces of information together with the mean IMF multiplicity for a given excitation energy shown in Fig. 8 (bottom) lead to a correlation between the mean IMF multiplicity and Z_{bound} with a maximum of 5.5 IMF's for $Z_{\text{bound}} \approx 35$. Although this is only a rough approximation, it shows that both the soft and the hard EOS do produce a number of IMF's which is comparable to the experimental findings if excitation energy is deposited into the QMD system. In line with the findings of Peilert and co-workers [25] we conclude that the discrepancies between the experiment and the QMD model cannot be attributed to an inability of the model in describing the fragment formation.

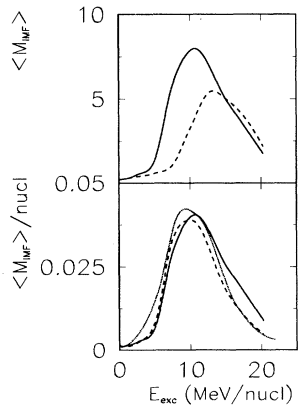

FIG. 8. Top: Correlation between the mean IMF multiplicity and the excitation energy per nucleon for a gold nucleus calculated using different EOS's: solid line, soft EOS; dashed line, hard EOS. Bottom: Correlation between the mean IMF multiplicity per nucleon and the excitation energy per nucleon for nuclei of different sizes calculated with a soft EOS: gold (solid line), xenon (dashed line), and zirconium (dotted line) nuclei. Within the errors the distributions are identical.

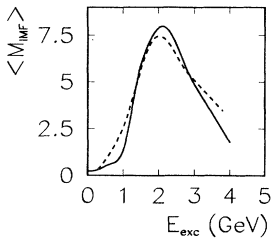

FIG. 9. Correlation between the mean IMF multiplicity and the excitation energy of a gold nucleus. The QMD results with soft EOS (solid line) are compared to those of the statistical model by Gross (dashed line).

C. Energy transfer during the collision

All the investigations discussed in Sec. V B indicate that in QMD events too little energy is transferred to the spectator matter. This energy transfer is governed by the elementary nucleon-nucleon cross section, which was assumed to be the same in the nuclear environment as in free space. In-medium modifications of the cross section are presently highly debated but so far no final conclusion has been reached whether they will increase or decrease the cross section. Therefore, our experimental findings may be a hint that the average momentum transfer in a single nucleon-nucleon collision is larger than expected from the free cross section. To settle this question, precise measurements of rapidity distributions of the particles from the participant zone are required.

VI. SUMMARY AND CONCLUSIONS

The fragmentation of gold nuclei on carbon, aluminum, copper, and lead targets at 600 MeV/nucleon was investigated with the ALADIN spectrometer. The multiplicity of IMF's produced in the decay of the projectile spectator as well as the multiplicity of light charged particles originating from the participant zone was compared to QMD calculations using both a soft and a hard EOS. The angular distributions of light charged particles from the reaction zone for all targets are very well reproduced by QMD calculations, the mean multiplicities are underestimated by about 20%. The production of IMF's, however, is significantly underestimated and a too large residual nucleus survives. Calculations with hard and soft EOS's result in a maximum mean IMF multiplicity of about 2 as compared to a measured value of 3.5.

To investigate whether this disagreement is caused by a deficiency in the description of the early collision phase of a heavy ion collision or of the subsequent fragment formation process, the time evolution of the system after a collision was studied within the QMD model. It was found that the fragment formation is completed within a time scale of about 100 fm/c and the remaining clusters are practically cold. In addition to the investigation of the collision process, the time evolution of an excited nucleus with a fixed excitation energy was studied. If equal amounts of excitation energies are assumed then QMD and statistical multifragmentation models yield comparable multiplicities for intermediate mass fragments which are compatible with the experimental findings. This is an indication that the underestimation of IMF production in a collision process is due to a lack of energy deposition in the spectator matter.

One of us (J.P.) acknowledges the financial support of the Deutsche Forschungsgemeinschaft.

[1] J. Hubele, P. Kreutz, J. C. Adloff, M. Begemann-Blaich, P. Bouissou, G. Imme, I. Iori, G. J. Kunde, S. Leray, V. Lindenstruth, Z. Liu, U. Lynen, R. J. Meijer, U. Milkau, A. Moroni, W. F. J. Müller, C. Ngô, C. A. Ogilvie, J. Pochodzalla, G. Raciti, G. Rudolf, H. Sann, A. Schüttauf, W. Seidel, L. Stuttge, W. Trautmann, and A. Tucholski, Z. Phys. A **340**, 263 (1991).

[2] D. R. Bowman, G. F. Peaslee, R. T. de Souza, N. Carlin, C. K. Gelbke, W. G. Gong, Y. D. Kim, M. A. Lisa, W. G. Lynch, L. Phair, M. B. Tsang, C. Williams, N. Colonna, K. Hanold, M. A. McMahan, G. J. Wozniak, L. G. Moretto, and W. A. Friedman, Phys. Rev. Lett. **67**, 1527 (1991).

[3] E. Piasecki, S. Bresson, B. Lott, R. Bougault, J. Colin, E. Crema, J. Galin, B. Gatty, A. Genoux-Lubain, D. Guerreau, D. Horn, D. Jacquet, U. Jahnke, J. Jastrzebski, A. Kordyasz, C. Le Brun, J. F. Lecolley, M. Louvel, M. Morjean, C. Paulot, L. Pienkowski, J. Pouthas, B. Quednau, W. U. Schröder, E. Schwinn, W. Skulski, and J. Töke, Phys. Rev. Lett. **66**, 1291 (1991).

[4] T. C. Sangster, H. C. Britt, D. J. Fields, L. F. Hansen, R. G. Lanier, M. N. Namboodiri, B. A. Remington, M. L. Webb, M. Begemann-Blaich, T. Blaich, M. M. Fowler, J. B. Wilhelmy, Y. D. Chan, A. Dacal, A. Harmon, J. Pouliot, R. G. Stokstad, S. Kaufman, F. Videbaek, Z. Fraenkel, G. Peilert, H. Stöcker, W. Greiner, A. Botvina, and I. N. Mishustin, Phys. Rev. C **46**, 1404 (1992).

[5] G. Bertsch and P. J. Siemens, Phys. Lett. **126B**, 9 (1983).

[6] C. J. Pethick and D. G. Ravenhall, Nucl. Phys. **A471**, 19c (1987).

[7] D. H. E. Gross and H. Massmann, Nucl. Phys. **A471**, 339c (1987).

[8] H. W. Barz, J. P. Bondorf, R. Donangelo, and H. Schulz, Phys. Lett. **169B**, 318 (1986).

[9] W. A. Friedman and W. G. Lynch, Phys. Rev. C **28**, 16 (1983).

[10] R. J. Charity, M. A. McMahan, G. L. Wozniak, R. J. McDonald, L. G. Moretto, D. G. Sarantites, L. G. Sobotka, G. Guarino, A. Pantaleo, L. Fiore, A. Gobbi, and K. D. Hildenbrand, Nucl. Phys. **A483**, 371 (1988).

[11] W. A. Friedman, Phys. Rev. Lett. **60**, 2125 (1988).

[12] W. A. Friedman, Phys. Rev. C **42**, 667 (1990).

[13] J. Hubele, P. Kreutz, V. Lindenstruth, J. C. Adloff, M. Begemann-Blaich, P. Bouissou, G. Imme, I. Iori, G. J. Kunde, S. Leray, Z. Liu, U. Lynen, R. J. Meijer, U. Milkau, A. Moroni, W. F. J. Müller, C. Ngô, C. A. Ogilvie, J. Pochodzalla, G. Raciti, G. Rudolf, H. Sann, A. Schüttauf, W. Seidel, L. Stuttge, W. Trautmann, A. Tucholski, R. Heck, A. R. DeAngelis, D. H. E. Gross, H. R. Jaqaman, H. W. Barz, H. Schulz, W. A. Friedman, and R. J. Charity, Phys. Rev. C **46**, R1577 (1992).

[14] P. Kreutz, J. C. Adloff, M. Begemann-Blaich, P. Bouissou, J. Hubele, G. Imme, I. Iori, G. J. Kunde, S. Leray, V. Lindenstruth, Z. Liu, U. Lynen, R. J. Meijer, U. Milkau, A. Moroni, W. F. J. Müller, C. Ngô, C. A. Ogilvie, J. Pochodzalla, G. Raciti, G. Rudolf, H. Sann, A. Schüttauf, W. Seidel, L. Stuttge, W. Trautmann, and A. Tucholski, Nucl. Phys. A (to be published).

[15] J. Aichelin and H. Stöcker, Phys. Lett. B **176**, 14 (1986).

[16] J. Aichelin, Phys. Rep. **202**, 233 (1991).

[17] D. H. Boal and J. N. Glosli, Phys. Rev. C **42**, R502 (1990).

[18] J. Cugnon, T. Mizutani, and J. Vandermeulen, Nucl. Phys. **A352**, 505 (1981).

[19] M. B. Tsang, G. F. Bertsch, W. G. Lynch, and M. Tohyama, Phys. Rev. C **40**, 1685 (1989).

[20] C. A. Ogilvie, J. C. Adloff, M. Begemann-Blaich, P. Bouissou, J. Hubele, G. Imme, I. Iori, P. Kreutz, G. J. Kunde, S. Leray, V. Lindenstruth, Z. Liu, U. Lynen, R. J. Meijer, U. Milkau, W. F. J. Müller, C. Ngô, J. Pochodzalla, G. Raciti, G. Rudolf, H. Sann, A. Schüttauf, W. Seidel, L. Stuttge, W. Trautmann, and A. Tucholski, Phys. Rev. Lett. **67**, 1214 (1991).

[21] For a recent review see D. H. E. Gross, Rep. Prog. Phys. **53**, 605 (1990).

[22] W. F. J. Müller, M. Begemann-Blaich, and J. Aichelin, Phys. Lett. B **298**, 27 (1993).

[23] J. Gosset, H. H. Gutbrod, W. G. Meyer, A. M. Poskanzer, A. Sandoval, R. Stock, and G. D. Westfall, Phys. Rev. C **16**, 629 (1977).

[24] W. Bauer, G. F. Bertsch, and S. Das Gupta, Phys. Rev. Lett. **58**, 863 (1987).

[25] G. Peilert, J. Konopka, H. Stöcker, W. Greiner, M. Blann, and M. G. Mustafa, Phys. Rev. C **46**, 1457 (1992).